

HEART RATE AND BLOOD PRESSURE DEPENDENCE OF AORTIC DISTENSIBILITY IN RATS: COMPARISON OF MEASURED AND CALCULATED PULSE WAVE VELOCITY

Bart SPRONCK, Isabella TAN, Koen D. REESINK, Dana GEORGEVSKY, Tammo DELHAAS, Alberto P. AVOLIO, and Mark BUTLIN

SUPPLEMENTAL DIGITAL CONTENT 1

Corresponding author

Bart Spronck, PhD

Dept. of Biomedical Engineering

School of Engineering & Applied Science

Yale University

New Haven, CT 06511

United States

E: bart.spronck@yale.edu

P: +1 203 432 6678

SUPPLEMENTAL METHODS

Diastolic foot detection for PWV_{TT} estimation

Foot detection was based on detection of the maximum second derivative of the respective blood pressure (BP) signals [1,2]. Second derivatives were obtained by filtering the signal twice using a finite impulse response (FIR) filter of width $2k$. $k = 1.5$ ms was chosen, consistent with our previous work [1]. To assess the sensitivity of the estimation of pulse wave velocity (PWV) as measured using pulse transit time (PWV_{TT}) on the choice of k , all analyses were also run for $k = 0.5$ ms and $k = 4.5$ ms. To further assess the sensitivity of our results on the method of foot detection, analyses were additionally performed using the intersecting tangent method.

Assessment of contractility

The first derivative of the aortic arch BP ($\frac{dP}{dt}_{\max}$) was computed as a measure of cardiac contractility.

Wave separation

Wave separation of the aortic arch BP signal ($P(t)$) was performed using a pressure-only method [3]. Forward and backward blood pressure waves ($P_f(t)$ and $P_b(t)$) were computed as

$$P_f(t) = (P(t) + Z_c \cdot Q(t))/2 , \quad (1)$$

$$P_b(t) = (P(t) - Z_c \cdot Q(t))/2 , \quad (2)$$

with Z_c the characteristic impedance and $Q(t)$ a triangular flow pattern with a duration of 30% of the ejection duration [3]. Ejection duration was determined as the time difference between the diastolic (minimum) point and the dicrotic notch, detected as the maximum second derivative after the systolic (maximum) point. As elaborated by Westerhof et al. [3], the magnitude of $Q(t)$ does not influence the wave separation; hence, a unit maximum was chosen. Z_c was computed in the frequency domain, and was taken to be the average of the 4th to the 7th harmonics of the input impedance modulus [3,4]. Finally, reflection index (RI) and reflection magnitude (RM) were calculated as

$$RI = \frac{|P_b|}{|P_b| + |P_f|} \quad \text{and} \quad RM = \frac{|P_b|}{|P_f|} , \quad (3)$$

with $|\dots|$ denoting the peak-to-trough amplitude.

Classes of data models

Data analysis was performed using the software package R 3.3.2 [5] using multilevel linear modelling as implemented in the nlme 3.1-128 package [6]. Note that multilevel linear modelling is capable of directly using the “raw” beat-to-beat data without applying any prior averaging. Least-squares means are obtained using the lsmeans function in the lsmeans 2.25 package [7].

Two classes of models were produced: models with heart rate (HR) as a categorical variable and models with HR as a continuous, linear variable. The former were used to generate plots and to study the effect of HR on dependent variables (PWV_{TT} , PWV as calculated from distensibility (PWV_{dist}), and BP parameters) without the assumption of HR having a linear effect on these parameters. The latter were used to quantify the effect of HR if linearity *is* assumed.

Statistical models with HR as a categorical predictor

These models contained the following fixed-effect terms:

1. An intercept,
2. An age term,
3. Four parameters modelling the effect of HR as a categorical variable on the dependent variable,
4. m parameters modelling the effect of BP (either mean arterial pressure (MAP) or diastolic blood pressure (DBP)) as a continuous variable through orthogonal polynomials, with m the highest order of the orthogonal polynomials (package polynom 1.3-9 [8]).
5. $4m$ parameters modelling the interaction of BP and HR.

Two levels of random effects are used: rat and HR category within rat.

For the between-rat variation, $m+1$ terms are used, modelling the intercept spread as well as the spread in the orthogonal polynomial coefficients. No correlation is assumed between the intercept and the polynomial coefficients.

For the within-rat variation between HRs, $m+1$ terms are used, again modelling the intercept spread as well as the spread in the orthogonal polynomial coefficients. No correlation is assumed between the intercept and the polynomial coefficients.

Residual variance is allowed to vary among rats and among HRs, involving $n+4$ parameters, where n is the number of rats for which the respective dependent variable was available ($n=17$ for PWV_{dist} ; $n=12$ for PWV_{TT} , RI, RM, and dP/dt_{max} ; and $n=24$ for systolic blood pressure (SBP), DBP, and MAP).

Statistical models with HR as a continuous predictor

These models differed to the models with HR as a categorical predictor only in terms of fixed-effect terms. The fixed-effects terms for the models with HR as a continuous predictor were:

1. An intercept,
2. An age term,
3. One parameter modelling the effect of HR on the dependent variable
4. m parameters modelling the effect of BP (either MAP or DBP) as a continuous variable through orthogonal polynomials, with m the highest order of the orthogonal polynomials.
5. m parameters modelling the interaction of BP and HR.

The random-effects terms were equal to those of the models with HR as a categorical predictor, as were the residual terms.

The statistical models with HR as a continuous predictor were used to estimate the linearised HR dependence of the dependent variables. p -values of this dependence (which can be expressed as a combination of mixed-effects model parameters) were obtained using the delta method, as implemented in the car 2.1-4 package [9].

Pressure-area curve models

Pressure-area curves are also modelled through multilevel modelling in a similar fashion to the PWV models described above. Area was modelled as a function of pressure, HR, and their interactions as described above. Again, both models with HR as a categorical as well as with HR as a continuous predictor were constructed. From these models describing area as a function of pressure, 'analytical'

distensibility-based PWV ($PWV_{\text{dist,ana}}$; Eq. 4) and its HR dependence were calculated using the delta method.

Choice of polynomial order (m)

In the aforementioned statistical models, quadratic orthogonal polynomials ($m=2$) were used to model BP. This choice was made since measurements were taken around three BP levels (MAP = 70, 100, and 130 mmHg). As such, a quadratic orthogonal polynomial could be uniquely and reliably parameterised. We have assessed performance of models incorporating higher-order polynomial terms (up to fourth order), but found that those models changed experimental results negligibly.

Correction for age

Multilevel models with different age corrections were compared based on the Bayesian information criterion (BIC). These included:

1. Models with age as an additive covariate.
2. Models with an age-HR interaction.
3. Models with an age-BP interaction.
4. Models with age-HR and age-BP interaction.
5. Models with an age-HR-BP interaction (second-order interaction).

For all dependent variables, option 1 (age as an additive covariate) yielded the lowest BIC, and as such was determined most appropriate.

Modelling assumptions

While fitting a mixed-effects models, the underlying distributional assumptions were carefully checked [10]. Independence of within-group errors was checked by plotting standardised residuals versus fitted values; normality of within-group errors was checked through q-q plots. Preliminary statistical models showed violation of homoscedasticity among rats and HRs; therefore, residual error variance was allowed to vary among rats and HRs. Normal distribution of random effects at both levels was checked through q-q plots. Homogeneity of the random effects distribution was ascertained by inspection of scatter plots of all combinations of random effects per level.

References

1. Tan I, Butlin M, Liu YY, Ng K, Avolio AP. Heart rate dependence of aortic pulse wave velocity at different arterial pressures in rats. *Hypertension* 2012; 60:528-533.
2. Chiu YC, Arand PW, Shroff SG, Feldman T, Carroll JD. Determination of pulse wave velocities with computerized algorithms. *Am Heart J* 1991; 121:1460-1470.
3. Westerhof BE, Guelen I, Westerhof N, Karemaker JM, Avolio A. Quantification of wave reflection in the human aorta from pressure alone: a proof of principle. *Hypertension* 2006; 48:595-601.
4. Nichols W, O'Rourke M, Vlachopoulos C. McDonald's blood flow in arteries: theoretical, experimental and clinical principles. London, United Kingdom: CRC press; 2011.
5. R Core Team. R: A Language and Environment for Statistical Computing. Vienna, Austria: R Foundation for Statistical Computing; 2016.
6. Pinheiro J, Bates D, DebRoy S, Sarkar D, R Core Team. nlme: Linear and Nonlinear Mixed Effects Models. 2016.
7. Lenth RV. Least-Squares Means: The R Package lsmeans. *Journal of Statistical Software* 2016; 69:1-33.
8. Venables B, Hornik K, Maechler M. polynom: A Collection of Functions to Implement a Class for Univariate Polynomial Manipulations. 2016.
9. Fox J, Weisberg S, Fox J. An R companion to applied regression. Thousand Oaks, Calif.: SAGE Publications; 2011.
10. Pinheiro JC, Bates DM. Mixed-Effects Models in S and S-PLUS. New York: Springer-Verlag; 2000.

SUPPLEMENTAL FIGURES

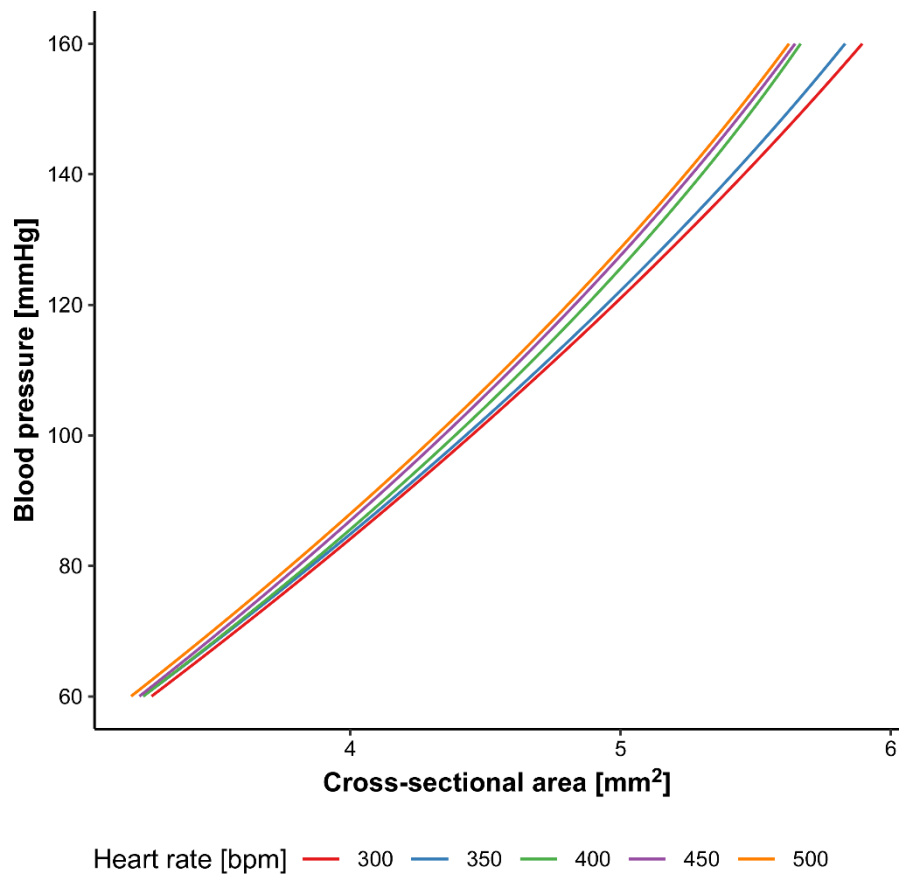


Figure S1. Averaged pressure–cross-sectional (P - A) area curves for different heart rates. Notice that, with an increase in heart rate, curves 1) shift leftward (towards smaller A), and also 2) show an increase in slope (dP/dA) as well as nonlinearity.

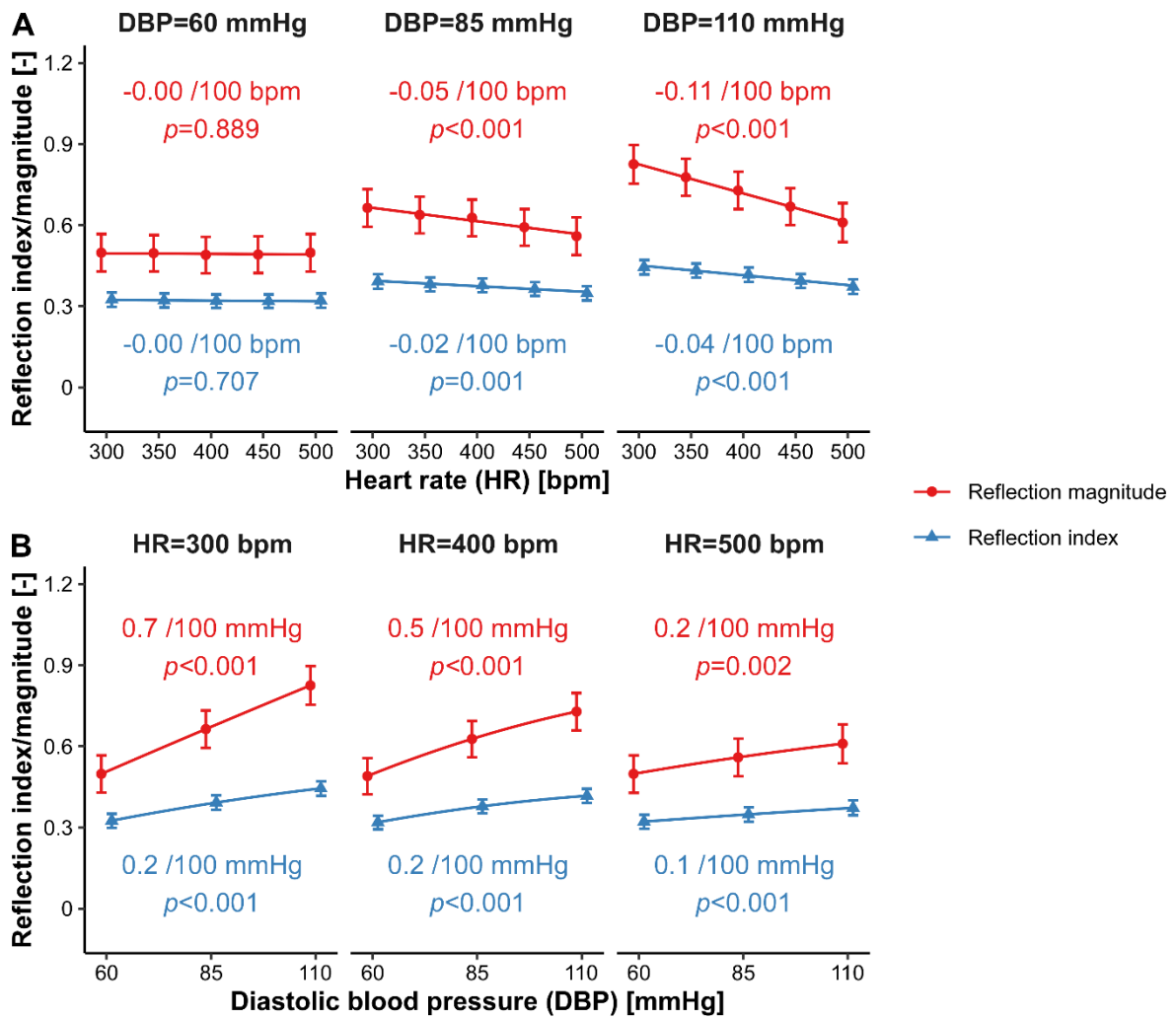


Figure S2. Reflection index and reflection magnitude as a function of diastolic blood pressure (**A**) and heart rate (**B**). Blood pressure dependences are calculated for a diastolic blood pressure of 85 mmHg. Points indicate mean \pm standard error.

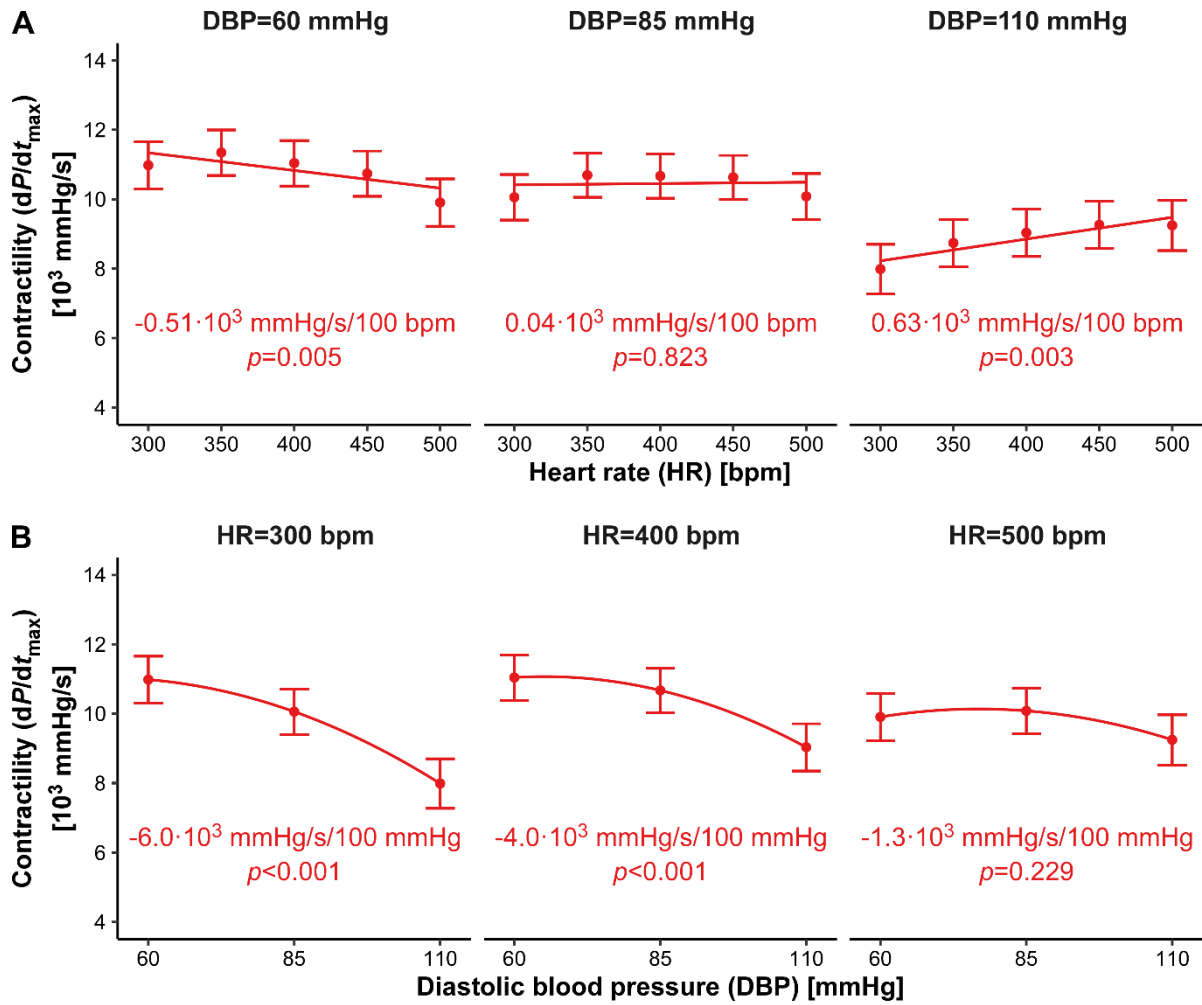


Figure S3. Contractility as a function of diastolic blood pressure (**A**) and heart rate (**B**). Blood pressure dependences are calculated for a diastolic blood pressure of 85 mmHg. Points indicate mean \pm standard error.

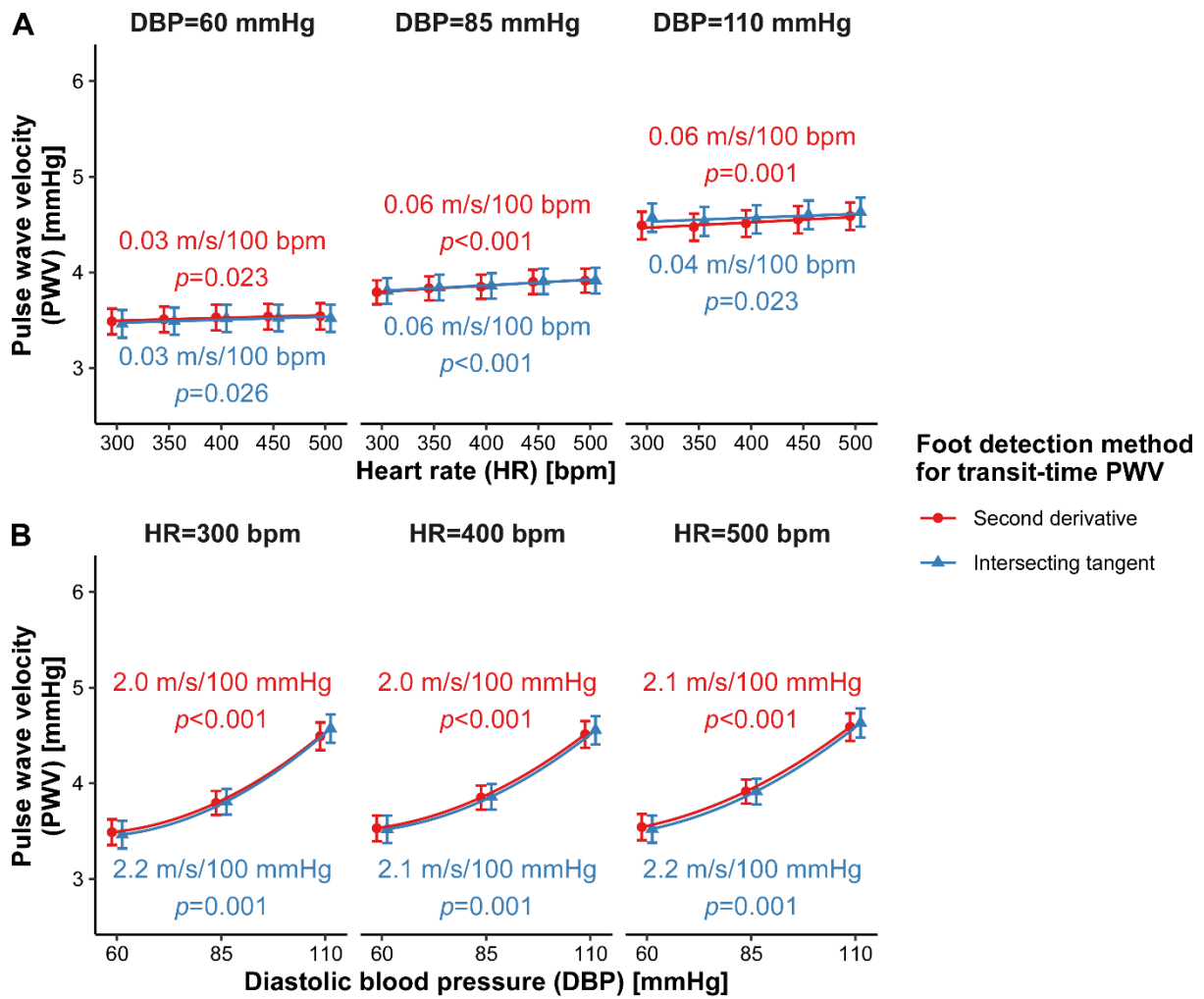


Figure S4. Comparison of intersecting tangent and second derivative foot detection methods for estimation of transit time pulse wave velocity. Blood pressure dependences are calculated for a diastolic blood pressure of 85 mmHg. Points indicate mean \pm standard error.

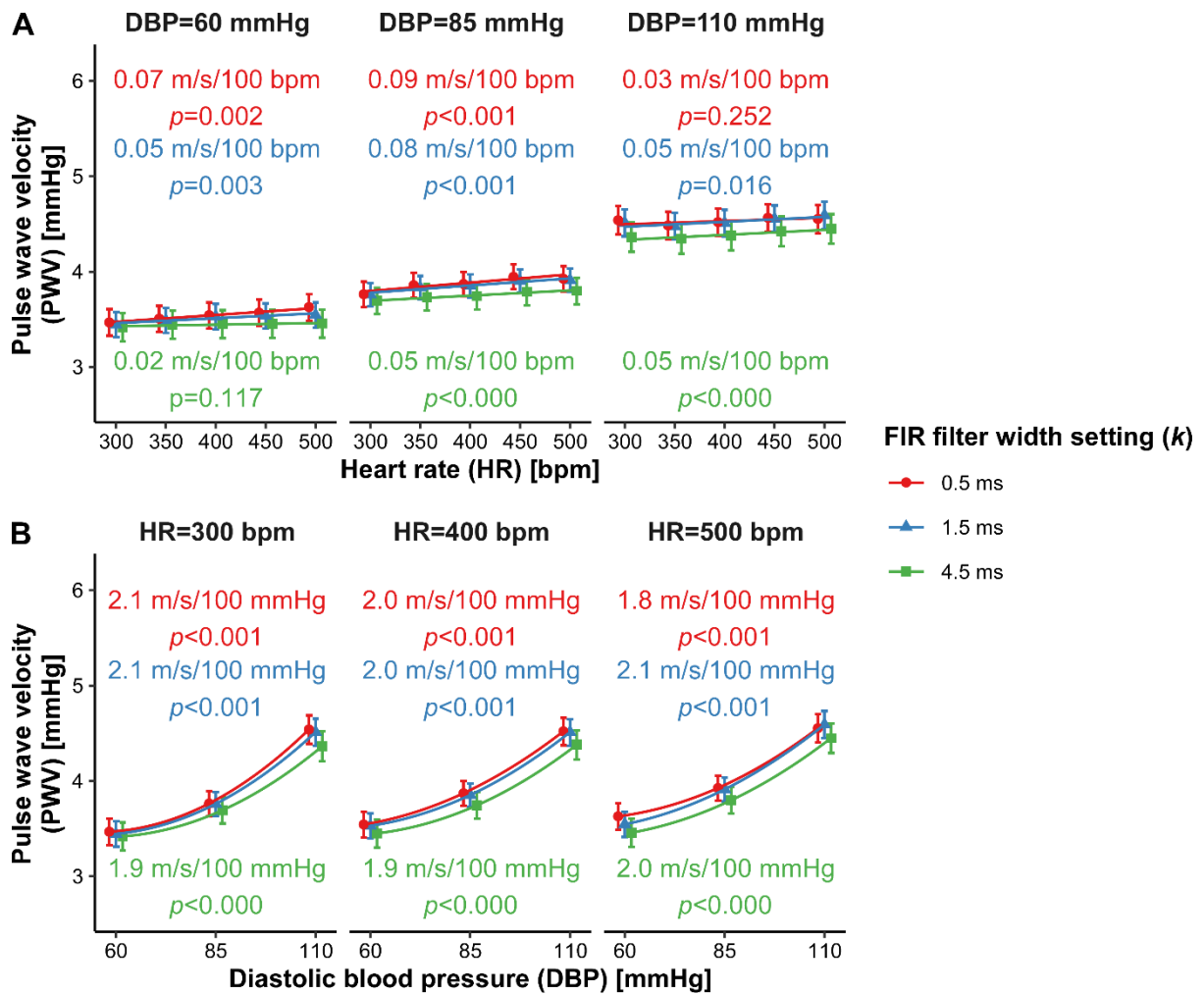


Figure S5. Influence of finite impulse response (FIR) filter width on estimation of transit time pulse wave velocity. Blood pressure dependences are calculated for a diastolic blood pressure of 85 mmHg. Points indicate mean \pm standard error.

SUPPLEMENTAL TABLES

Table S1. Statistical comparison of heart rate dependences at different mean arterial pressures.

	PWV _{TT}		
	70 mmHg	100 mmHg	130 mmHg
70 mmHg	-	0.11	0.16
100 mmHg	<0.001	-	0.05
130 mmHg	<0.001	0.005	-

	PWV _{dist}		
	70 mmHg	100 mmHg	130 mmHg
70 mmHg	-	0.09	0.02
100 mmHg	0.070	-	-0.08
130 mmHg	0.813	0.114	-

Above diagonals: differences in linear trend slope values, in m/s/100 bpm. Below diagonal: corresponding p -values. Slope values are printed in boldface when their corresponding $p < 0.05$. PWV_{TT}, transit-time pulse wave velocity; PWV_{dist}, distensibility-calculated pulse wave velocity.

Table S2. Statistical comparison of mean arterial pressure dependences at different heart rates.

		PWV _{TT}				
		300 bpm	350 bpm	400 bpm	450 bpm	500 bpm
300 bpm	-	0.1	0.2	0.4	0.5	
350 bpm	0.213	-	0.1	0.3	0.4	
400 bpm	0.005	0.078	-	0.2	0.3	
450 bpm	0.000	0.000	0.012	-	0.1	
500 bpm	0.000	0.000	0.001	0.148	-	

		PWV _{dist}				
		300 bpm	350 bpm	400 bpm	450 bpm	500 bpm
300 bpm	-	0.1	0.2	0.1	0.1	
350 bpm	0.772	-	0.1	-0.0	0.0	
400 bpm	0.455	0.635	-	-0.1	-0.1	
450 bpm	0.802	0.967	0.605	-	0.0	
500 bpm	0.759	0.986	0.647	0.953	-	

Above diagonals: differences in linear trend slope values, in m/s/100 mmHg, evaluated at a mean arterial pressure of 100 mmHg. Below diagonal: corresponding p -values. Slope values are printed in boldface when their corresponding $p < 0.05$. PWV_{TT}, transit-time pulse wave velocity; PWV_{dist}, distensibility-calculated pulse wave velocity.

Table S3. Statistical comparison of heart rate dependences at different diastolic blood pressures.

	PWV _{TT}		
	60 mmHg	85 mmHg	110 mmHg
60 mmHg	-	0.03	0.03
85 mmHg	0.011	-	0.01
110 mmHg	0.209	0.717	-

	PWV _{dist}		
	60 mmHg	85 mmHg	110 mmHg
60 mmHg	-	0.00	-0.13
85 mmHg	0.953	-	-0.13
110 mmHg	0.077	0.023	-

	PWV _{dist,ana}		
	60 mmHg	85 mmHg	110 mmHg
60 mmHg	-	0.02	0.04
85 mmHg	0.429	-	0.02
110 mmHg	0.384	0.353	-

Above diagonals: differences in linear trend slope values, in m/s/100 bpm. Below diagonal: corresponding p -values. Slope values are printed in boldface when their corresponding $p < 0.05$. PWV_{TT}, transit-time pulse wave velocity; PWV_{dist}, distensibility-calculated pulse wave velocity; PWV_{dist,ana}, ‘analytical’ distensibility-based pulse wave velocity.

Table S4. Statistical comparison of diastolic blood pressure dependences at different heart rates.

		PWV _{TT}				
		300 bpm	350 bpm	400 bpm	450 bpm	500 bpm
300 bpm	-	-0.1	-0.0	0.0	0.1	
350 bpm	0.401	-	0.0	0.1	0.2	
400 bpm	0.626	0.681	-	0.1	0.1	
450 bpm	0.812	0.210	0.399	-	0.1	
500 bpm	0.442	0.104	0.191	0.516	-	

		PWV _{dist}				
		300 bpm	350 bpm	400 bpm	450 bpm	500 bpm
300 bpm	-	-0.5	-0.4	-0.5	-0.7	
350 bpm	0.142	-	0.1	-0.0	-0.2	
400 bpm	0.279	0.687	-	-0.2	-0.3	
450 bpm	0.117	0.921	0.614	-	-0.1	
500 bpm	0.051	0.619	0.367	0.690	-	

		PWV _{dist,ana}				
		300 bpm	350 bpm	400 bpm	450 bpm	500 bpm
300 bpm	-	0.1	0.3	0.2	0.2	
350 bpm	0.501	-	0.2	0.0	0.0	
400 bpm	0.110	0.315	-	-0.1	-0.1	
450 bpm	0.388	0.822	0.451	-	0.0	
500 bpm	0.383	0.817	0.452	0.996	-	

Above diagonals: differences in linear trend slope values, in m/s/100 mmHg, evaluated at a diastolic blood pressure of 85 mmHg. Below diagonal: corresponding p -values. PWV_{TT}, transit-time pulse wave velocity; PWV_{dist}, distensibility-calculated pulse wave velocity; PWV_{dist,ana}, 'analytical' distensibility-based pulse wave velocity.